

MICROCOPY RESOLUTION TEST CHART
NATIONAL BUREAU OF STANDARDS-1963-A

ADA 130631

2

AD



**CHEMICAL
SYSTEMS
LABORATORY**

US Army Armament Research and Development Command
Aberdeen Proving Ground, Maryland 21010

CONTRACTOR REPORT ARCSL-CR-83039

**FORWARD MULTIPLE SCATTERING CORRECTIONS
AS FUNCTION OF DETECTOR FIELD OF VIEW**

by

Andrew Zardecki

Adarsh Deepak

June 1983

**Institute for Atmospheric Optics and Remote Sensing (IFAORS)
P. O. Box P
Hampton, Virginia 23666**

Contract No. DAAK 11-79-0100



**DTIC
SELECTED
JUL 25 1983**

DTIC FILE COPY

Approved for public release; distribution unlimited.

88 07 22 086

Disclaimer

The views, opinions and/or findings contained in this report are those of the authors and should not be construed as an official Department of the Army position, policy, or decision unless so designated by other documentation.

Disposition

Destroy this report when it is no longer needed. Do not return to the originator.

UNCLASSIFIED

SECURITY CLASSIFICATION OF THIS PAGE (When Data Entered)

REPORT DOCUMENTATION PAGE		READ INSTRUCTIONS BEFORE COMPLETING FORM
1. REPORT NUMBER ARCSL-CR-83039	2. GOVT ACCESSION NO. AD-A130631	3. RECIPIENT'S CATALOG NUMBER
4. TITLE (and Subtitle) FORWARD MULTIPLE SCATTERING CORRECTIONS AS FUNCTION OF DETECTOR FIELD OF VIEW		5. TYPE OF REPORT & PERIOD COVERED DAAK 11-79-0100 C-
		6. PERFORMING ORG. REPORT NUMBER IFAORS-146
7. AUTHOR(s) Andrew Zardecki Adarsh Deepak		8. CONTRACT OR GRANT NUMBER(s) 1L162622A552
9. PERFORMING ORGANIZATION NAME AND ADDRESS Institute for Atmospheric Optics and Remote Sensing (IFAORS) P. O. Box P Hampton, Virginia 23666		10. PROGRAM ELEMENT, PROJECT, TASK AREA & WORK UNIT NUMBERS
11. CONTROLLING OFFICE NAME AND ADDRESS Commander, Chemical Systems Laboratory ATTN: DRDAR-CLJ-R Aberdeen Proving Ground, Maryland 21010		12. REPORT DATE June 1983
		13. NUMBER OF PAGES 40
14. MONITORING AGENCY NAME & ADDRESS (if different from Controlling Office) Commander, Chemical Systems Laboratory ATTN: DRDAR-CLB-PO Aberdeen Proving Ground, Maryland 21010		15. SECURITY CLASS. (of this report) UNCLASSIFIED
		15a. DECLASSIFICATION/DOWNGRADING SCHEDULE NA
16. DISTRIBUTION STATEMENT (of this Report) Approved for public release; distribution unlimited.		
17. DISTRIBUTION STATEMENT (of the abstract entered in Block 20, if different from Report)		
18. SUPPLEMENTARY NOTES Contract Project Officer: Dr. G. Holst (DRDAR-CLB-PO, 301-671-2543)		
19. KEY WORDS (Continue on reverse side if necessary and identify by block number) Forward multiple scattering Optical extinction measurements Multiple scattering effects Backscattering Aerosol particles Electro-optical systems Detector field of view		
20. ABSTRACT (Continue on reverse side if necessary and identify by block number) The theoretical formulations are given for an approximate method based on the solution of the radiative transfer equation in the small angle approximation. The method is approximate in the sense that an approximation is made in addition to the small angle approximation. Numerical results were obtained for multiple scattering effects as functions of the detector field of view as well as the size of the detector's aperture for three different values of the optical depth (τ) (= 1.0, 4.0 and 10.0). Three cases of aperture size were considered -- namely, equal to or (Cont'd on reverse side)		

UNCLASSIFIED

SECURITY CLASSIFICATION OF THIS PAGE (When Data Entered)

UNCLASSIFIED

SECURITY CLASSIFICATION OF THIS PAGE(When Data Entered)

20. **ABSTRACT (Cont'd)**

smaller or larger than the laser beam diameter. The contrast between the on-axis intensity and the received power for the last three cases is clearly evident.

UNCLASSIFIED

SECURITY CLASSIFICATION OF THIS PAGE(When Data Entered)

BLANK

CONTENTS

	Page
1. INTRODUCTION.....	7
2. THE FANTE-DOLIN THEORY.....	8
3. CASE OF COLLIMATED GAUSSIAN BEAM.....	12
4. CASE OF GENERAL GAUSSIAN BEAM.....	14
5. RESULTS AND DISCUSSIONS.....	15
6. RECOMMENDATIONS.....	26
LITERATURE CITED.....	33
DISTRIBUTION.....	35

FIGURE CAPTIONS

Figure

1	Normalized intensity on the beam axis as function of detector FOV corresponding to $\alpha = 46.80 \text{ rad}^{-1}$, $R_D = 1.0 \text{ cm}$, and $\tau = 1.0$	10
2	Normalized intensity on the beam axis as function of detector FOV corresponding to $\alpha = 46.80 \text{ rad}^{-1}$, $R_D = 1.0 \text{ cm}$, and $\tau = 4.0$	16
3.	Normalized intensity on the beam axis as function of detector FOV corresponding to $\alpha = 46.80 \text{ rad}^{-1}$, $R_D = 1.0 \text{ cm}$, and $\tau = 10.0$	17
4.	Received power (arbitrary units) on the beam axis as function of detector FOV corresponding to $\alpha = 46.80 \text{ rad}^{-1}$, $R_D = 1.0 \text{ cm}$, and $\tau = 1.0$	19
5.	Received power (arbitrary units) on the beam axis as function of detector FOV corresponding to $\alpha = 46.80 \text{ rad}^{-1}$, $R_D = 1.0 \text{ cm}$, and $\tau = 4.0$	20
6.	Received power (arbitrary units) on the beam axis as function of detector FOV corresponding to $\alpha = 46.80 \text{ rad}^{-1}$, $R_D = 1.0 \text{ cm}$, and $\tau = 10.0$	21
7.	Normalized intensity on the beam axis as function of detector FOV corresponding to $\alpha = 289.33 \text{ rad}^{-1}$, $R_D = 1.0 \text{ cm}$, and $\tau = 1.0$	22

Figure	Page
8. Normalized intensity on the beam axis as function of detector FOV corresponding to $\alpha = 289.33 \text{ rad}^{-1}$, $R_D = 1.0 \text{ cm}$, and $\tau = 4.0$	23
9. Normalized intensity on the beam axis as function of detector FOV corresponding to $\alpha = 289.33 \text{ rad}^{-1}$, $R_D = 1.0 \text{ cm}$, and $\tau = 10.0$	24
10. Received power (arbitrary units) on the beam axis as function of detector FOV corresponding to $\alpha = 289.33 \text{ rad}^{-1}$, $R_D = 1.0 \text{ cm}$, and $\tau = 4.0$. Received power is multiplied by $\exp(\tau)$	25
11. Normalized intensity on the beam axis as function of detector FOV for the same parameters as in Fig. 8 except $R_D = 0.2 \text{ cm}$	27
12. Received power (arbitrary units) on the beam axis as a function of detector FOV, for the same parameters as in Fig. 11. The received power is multiplied by $\exp(\tau)$	28
13. Normalized intensity on the beam axis as function of detector FOV for the same parameters as in Fig. 8 except $R_D = 2.0 \text{ cm}$	29
14. Received power (arbitrary units) on the beam axis as a function of detector FOV, for the same parameters as in Fig. 13. The received power is multiplied by $\exp(\tau)$	30

FORWARD MULTIPLE SCATTERING CORRECTIONS
AS FUNCTION OF DETECTOR FIELD OF VIEW

I. INTRODUCTION

Low visibility atmospheric conditions occur in the presence of heavy concentrations of atmospheric aerosols such as dust, smoke and fog. Scattering of laser radiation by such aerosol clouds, being basically a multiple scattering process, is very difficult to predict. A fruitful approach to the problem has been a Monte Carlo technique, because it can handle strange geometries as well as inhomogeneities¹⁻³. Recently, considerable attention has been paid to analytical solutions to the equation of transfer in a form appropriate for the laser beam propagation problem⁴⁻⁹. Although exact solutions have not been obtained to date, there are some special cases where simple and useful approximate solutions to the equation of transfer are available. For tenuous distribution of scatterers, the first-order multiple scattering theory can be used, and for dense distribution the diffusion approximation is appropriate. If the particle size is large compared with incident wavelength, the energy scattered by the particle is largely confined within a small angle in the forward direction and, therefore, by employing the small-angle approximation it is possible to simplify the equation of transfer. In Ref. 8, a systematic study of contributions of increasing order of scattering for both realistic and model aerosols has been conducted.

As indicated by Ishimaru^{10,11}, the first-order multiple scattering approximation is applicable when the density of scatterers is so low that the diffuse (incoherent) intensity is considerably smaller than the reduced (coherent) intensity. This will certainly be the case if optical distance traversed by the beam is much smaller than unity. However, the same weak fluctuation case is also encountered in the situations where the receiver has a narrow receiving angle. In this case, the amount of scattered intensity entering into the receiver is small compared with the direct coherent intensity, and therefore the received field is predominantly coherent. The effect of the detector's finite field of view on the received power has been a subject of comprehensive investigations related to forward scattering corrections for optical extinction measurements¹²⁻¹⁷.

The purpose of this paper is to study the effect of a finite field of view on the intensity and the received power of a laser beam undergoing multiple scattering. Our analytic approach is based on the theory of Dolin¹⁸ and Fante¹⁹⁻²², summarized in Section II. In Sections II and IV, we apply this theory to Gaussian beams. Numerical results relevant to the beam propagation in a water cloud and model aerosol particles are presented in Section V.

II. THE FANTE-DOLIN THEORY

Our considerations will be based on the equation of radiative transfer for the radiance (specific intensity) distribution function, $I(\vec{\phi}, \vec{r}, z)$. In the small angle approximation, $I(\vec{\phi}, \vec{r}, z)$ satisfies

$$\vec{\phi} \cdot \frac{\partial I}{\partial \vec{r}} + \frac{\partial I}{\partial z} + \sigma I = \sigma_s \int P(\vec{\phi} - \vec{\phi}') I(\vec{\phi}', \vec{r}, z) d\vec{\phi}' \quad (1)$$

where σ and σ_s are volume extinction and scattering coefficients (m^{-1}) for the aerosol medium; \vec{r} is the component of the position vector transverse to the z axis; and $\vec{\phi}$ is the transverse component of the unit propagation vector (Fig. 1 in Refs. 8 and 9).

In the work of Dolin¹⁸ and Fante¹⁹⁻²², which applies to sharply peaked phase functions, $I(\vec{\phi}', \vec{r}, z)$ in the integrand on the right hand side of Eq. (1) is expanded in Taylor series about $\vec{\phi}' = \vec{\phi}$. More precisely, $I(\vec{\phi}', \vec{r}, z)$ is split into

$$I(\vec{\phi}', \vec{r}, z) = I^{(0)}(\vec{\phi}, \vec{r}, z) + I^{(s)}(\vec{\phi}, \vec{r}, z) \quad (2)$$

where superscripts 0 and s refer to unscattered and scattered radiance, respectively. Then, one expands

$$\begin{aligned} I^{(s)}(\vec{\phi}', \vec{r}, z) &= I^{(s)}(\vec{\phi}, \vec{r}, z) \\ &+ \sum_k (\phi' - \phi)_k \frac{\partial}{\partial \phi_k} I^{(s)}(\vec{\phi}, \vec{r}, z) \\ &+ \frac{1}{2} \sum_k \sum_l (\phi' - \phi)_k (\phi' - \phi)_l \frac{\partial^2}{\partial \phi_k \partial \phi_l} I^{(s)}(\vec{\phi}, \vec{r}, z) + \dots \end{aligned} \quad (3)$$

where k and l refer to the Cartesian components of the $\vec{\phi}$ vector. Recall that $\vec{\phi} = \phi_x \hat{x} + \phi_y \hat{y}$.

Equation (1) now yields

$$\vec{\phi} \cdot \frac{\partial I^{(0)}}{\partial \vec{r}} + \frac{\partial I^{(0)}}{\partial z} + \sigma I^{(0)} = 0 \quad (4)$$

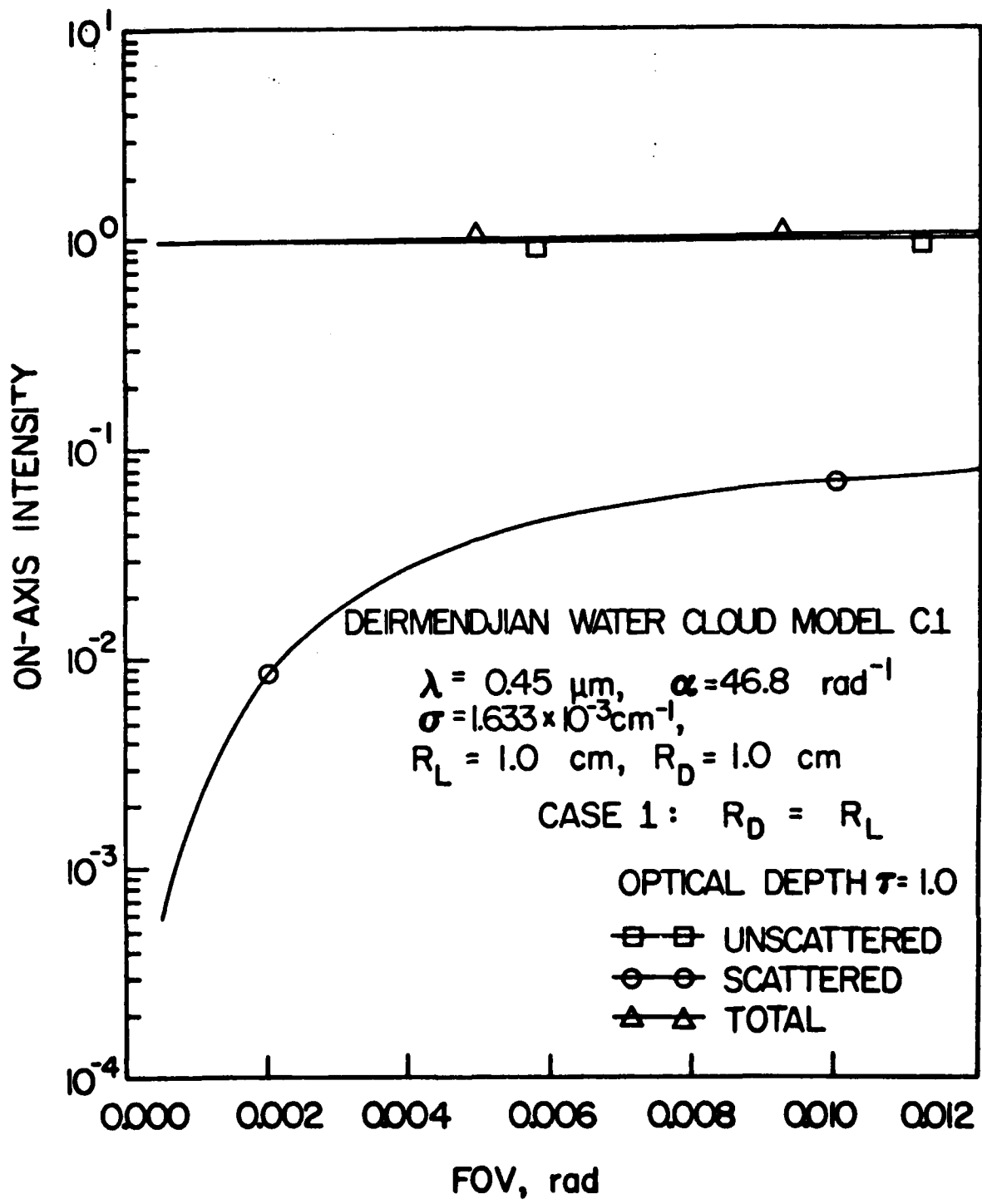


Figure 1. Normalized intensity on the beam axis as function of detector FOV corresponding to $\alpha = 46.80 \text{ rad}^{-1}$, $R_D = 1.0 \text{ cm}$, and $\tau = 1.0$.

while $I^{(s)}$ is determined from the nonhomogeneous equation

$$\vec{\phi} \cdot \frac{\partial I^{(s)}}{\partial \vec{r}} - \frac{\sigma\omega}{4} \langle \vec{\phi}^2 \rangle \nabla_{\vec{\phi}}^2 I^{(s)} + \frac{\partial I^{(s)}}{\partial z} + \sigma(1-\omega) I^{(s)} = \sigma\omega \int P(\vec{\phi} - \vec{\phi}') I^{(o)}(\vec{\phi}', \vec{r}, z) d^2\phi' \quad (5)$$

where $\omega = \sigma_s/\sigma$ is the single scattering albedo; and $\langle \vec{\phi}^2 \rangle$ is defined as

$$\langle \vec{\phi}^2 \rangle = \int P(\vec{\phi}) \vec{\phi}^2 d^2\phi \quad (6)$$

In deriving Eq. (5) we have neglected the terms of higher order than second in Eq. (3). The solutions to Eqs. (4) and (5) can be obtained by the method of characteristics in the Fourier space of the variables $\vec{\phi}$ and \vec{r} . With the Fourier transforms defined generically as

$$\hat{I}(\vec{\xi}, \vec{\eta}, z) = \iint_{-\infty}^{\infty} d^2\phi d^2r I(\vec{\phi}, \vec{r}, z) e^{i(\vec{\xi} \cdot \vec{\phi} + \vec{\eta} \cdot \vec{r})} \quad (7)$$

$$\hat{P}(\vec{\xi}) = \int_{-\infty}^{\infty} d^2\phi P(\vec{\phi}) e^{i\vec{\xi} \cdot \vec{\phi}} \quad (8)$$

we obtain the following solutions

$$\hat{I}^{(o)}(\vec{\xi}, \vec{\eta}, z) = \hat{I}(\vec{\xi} + \vec{\eta}z, \vec{\eta}, z=0) e^{-\sigma z} \quad (9)$$

and

$$\hat{I}^{(s)}(\vec{\xi}, \vec{\eta}, z) = \hat{I}(\vec{\xi} + \vec{\eta}z, \vec{\eta}, z=0) \int P(\vec{\xi} + \vec{\eta}(z-z')) e^{-\sigma z} \cdot \exp \left\{ - \int_z^z \left[\frac{\sigma\omega}{4} \langle \vec{\phi}^2 \rangle |\vec{\xi} + \vec{\eta}(z-z'')|^2 + \sigma(1-\omega) \right] dz'' \right\} dz' \quad (10)$$

for the unscattered and scattered contributions, respectively.

III. CASE OF COLLIMATED GAUSSIAN BEAM

We assume now that in the single scattering theory the scattering phase function $P(\vec{\phi})$ is given by a Gaussian function, i.e.,

$$P(\vec{\phi}) = \frac{\gamma^2}{\pi} \exp(-\alpha^2 \vec{\phi}^2) \quad (11)$$

and that the incident collimated beam, directed along the z axis, has a Gaussian spatial form, i.e.,

$$I(\vec{\phi}, \vec{r}, z=0) = F_0 \pi^{-1} \gamma^2 \delta^{(2)}(\vec{\phi}) \exp(-\gamma^2 \vec{r}^2) \quad (12)$$

where $\delta^{(2)}$ is the Dirac delta function.

In the situation modeled by Eqs. (11) and (12), we obtain, after performing the inverse Fourier transforms of Eqs. (9) and (10), the explicit formulas for $I^{(0)}(\vec{\phi}, \vec{r}, z)$ and $I^{(s)}(\vec{\phi}, \vec{r}, z)$. They read

$$I^{(0)}(\vec{\phi}, \vec{r}, z) = F_0 \pi^{-1} e^{-\sigma z} e^{-\gamma^2 \vec{r}^2} \delta^{(2)}(\vec{\phi}) \quad (13)$$

and

$$I^{(s)}(\vec{\phi}, \vec{r}, z) = \frac{F_0 \sigma \omega e^{-\sigma z}}{(2\pi)^2} \int dz' [4A(z')C(z') - B^2(z')]^{-1} \cdot \exp\left\{-\frac{A(z')\vec{r}^2 - 2\mathfrak{B}(z')\vec{\phi}\cdot\vec{r} + C(z')\vec{\phi}^2}{4A(z')C(z') - B^2(z')}\right\} e^{i\omega z'} \quad (14)$$

where the functions A , B , and C are defined as

$$\begin{aligned} A(z') &= \frac{1 + \sigma \omega z'}{4\alpha^2} \\ B(z') &= \frac{2z' + \sigma \omega z'^2}{4\alpha^2} \\ C(z') &= \frac{1}{4\gamma^2} + \frac{z'^2 + \sigma \omega z'^3/3}{4\alpha^2} \end{aligned} \quad (15)$$

In polar coordinates (θ, b) , the vector $\vec{\phi}$ can be expressed by

$$\begin{aligned}\phi_x &= \theta \cos b \\ \phi_y &= \theta \sin b\end{aligned}\tag{16}$$

For a detector having the field of view (FOV) half-angle, θ_D , the received intensity is obtained from Eq. (14) after integration over the angle b in the range $(0, 2\pi)$ and over θ in the range $(0, \theta_D)$. The received intensity $F^{(s)}(\theta_D, \vec{r}, \sigma z)$ corresponding to the scattered beam thus becomes

$$F^{(s)}(\theta_D, \vec{r}, \sigma z) = \int_0^{\theta_D} I^{(s)}(\theta, \vec{r}, \sigma z) \theta \, d\theta\tag{17}$$

where

$$\begin{aligned}I^{(s)}(\theta, \vec{r}, \sigma z) &= \frac{F_0 \omega e^{-\sigma z}}{2\pi} \int_0^{\sigma z} [4A\left(\frac{x}{\sigma}\right)C\left(\frac{x}{\sigma}\right) - B^2\left(\frac{x}{\sigma}\right)]^{-1} \\ &\cdot I_0 \left[\frac{\theta r B(x/\sigma)}{4A(x/\sigma)C(x/\sigma) - B^2(x/\sigma)} \right] \\ &\cdot \exp \left[-\frac{A(x/\sigma)r^2 + C(x/\sigma)\theta^2}{4A(x/\sigma)C(x/\sigma) - B^2(x/\sigma)} \right] e^{\omega x} \, dx\end{aligned}\tag{18}$$

Here I_0 is the modified Bessel function of zeroth order, and x is a dimensionless integration variable.

The contribution coming from the unscattered part of the beam is

$$F^{(o)}(\theta_D, \vec{r}, \sigma z) = F_0 \pi^{-1} e^{-\sigma z} e^{-\gamma^2 r^2}\tag{19}$$

It is thus seen that the numerical results can be extracted from this theory in a rather simple manner by performing merely a double integration.

IV. CASE OF GENERAL GAUSSIAN BEAM

More generally, one can account both for the spatial and angular divergence of the laser beam assuming a Gaussian law of the form

$$I(\vec{\phi}, \vec{r}, z=0) = F_0 \beta^2 \gamma^2 \pi^{-2} \exp(-\beta^2 \phi^2 - \gamma^2 r^2) \quad (20)$$

for the incident beam. Here, the parameter β describes the angular divergence.

By following exactly the same line of reasoning as in Section III, we obtain the following contributions $F^{(s)}(\theta_D, \vec{r}, \sigma z)$ corresponding to the scattered beam, viz.,

$$F^{(s)}(\theta_D, \vec{r}, \sigma z) = \theta_D^2 \int_0^1 I^{(s)}(\theta' \theta_D, \vec{r}, \sigma z) \theta' d\theta' \quad (21)$$

where

$$\begin{aligned} I^{(s)}(\theta, \vec{r}, \sigma z) &= F_0 \omega \sigma z e^{-\sigma z / 2\pi} \\ &+ \int_0^1 \left[4A\{(x/\sigma) z\} C\{(x/\sigma) z\} - B^2\{(x/\sigma) z\} \right]^{-1} \\ &+ I_0 \left[\frac{\theta(\gamma \vec{r}) - B\{(x/\sigma) z\}/\gamma}{4A\{(x/\sigma) z\} C\{(x/\sigma) z\} - B^2\{(x/\sigma) z\}} \right] \\ &+ \exp \left[- \frac{(\gamma \vec{r})^2 A\{(x/\sigma) z\}/\gamma^2 + C\{(x/\sigma) z\} \theta^2}{4A\{(x/\sigma) z\} C\{(x/\sigma) z\} - B^2\{(x/\sigma) z\}} \right] \\ &+ \exp(\omega x \sigma z) \cdot dx' \end{aligned} \quad (22)$$

and I_0 is the modified Bessel function of zeroth order.

For the unscattered beam, we obtain

$$\begin{aligned}
 F^{(0)}(\theta_D, \gamma r, \sigma z) &= 2F_0 \beta^2 \exp(-\sigma z) \theta_D^2 / \pi \\
 &+ \int_0^1 \theta' d\theta' I_0 \{ 2(\gamma/\sigma) \theta_D \theta' (\gamma r) \sigma z \} \\
 &+ \exp \{ -(\gamma r)^2 - [(\gamma/\sigma)^2 (\sigma z)^2 + \beta^2] \theta_D^2 \theta'^2 \} \quad (23)
 \end{aligned}$$

The integrals in Eqs. (22) and (23) have limits 0 and 1. This choice of limits anticipates the use of Gaussian quadrature in numerical computation.

V. RESULTS AND DISCUSSIONS

The numerical values were obtained for the on-axis intensities as a function of θ_D , and the plots shown in Figs. 1-3 depict the unscattered (reduced) intensity (squares), scattered or diffuse intensity (circles), and total intensity (triangles) on the beam axis for optical depth $\tau = 1, 4,$ and $10,$ respectively. A divergent beam with the parameters $\beta = 2\pi/(\gamma\lambda)$ and $\gamma = 1.0 \text{ cm}^{-1}$ is assumed to be propagating with the Deirmendjian water cloud²⁴ model C1. For $\lambda = 0.45 \text{ }\mu\text{m}$, the extinction coefficient is obtained from the Mie theory computations when a modified gamma distribution is taken from water cloud particle size distribution. One also obtained $\alpha = 46.80 \text{ rad}^{-1}$ for the Gaussian fit to the phase function. For a coaxial detector, with a diameter $R_D = 1.0 \text{ cm}$, the same as the laser beam diameter, the intensity F becomes a function of θ_D and z . We normalize the intensities by dividing

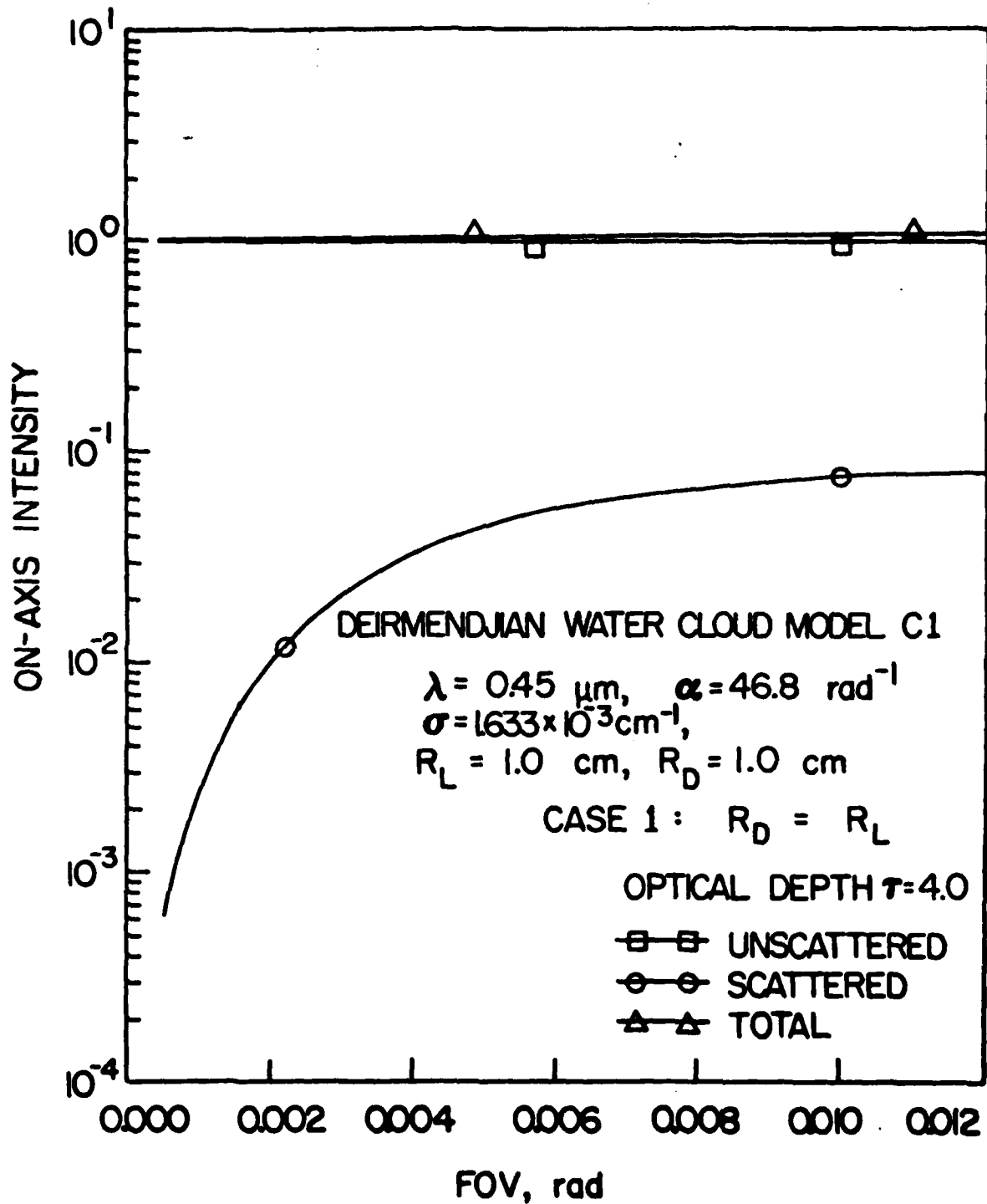


Figure 2. Normalized intensity on the beam axis as function of detector FOV corresponding to $\alpha = 46.80 \text{ rad}^{-1}$, $R_D = 1.0 \text{ cm}$, and $\tau = 4.0$.

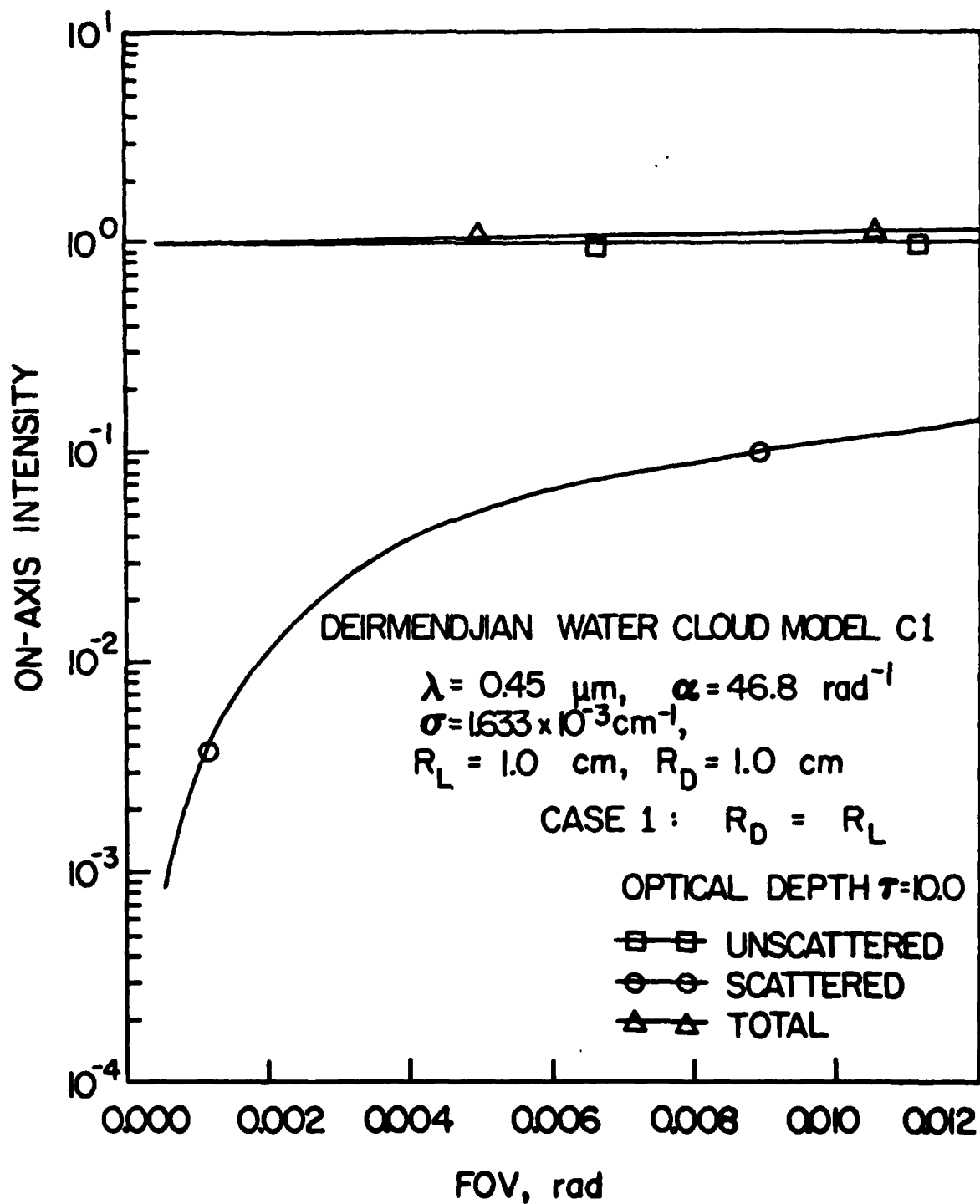


Figure 3. Normalized intensity on the beam axis as function of detector FOV corresponding to $\alpha = 46.80 \text{ rad}^{-1}$, $R_D = 1.0 \text{ cm}$, and $\tau = 10.0$.

out the factor $F^{(0)}(\theta_D = \infty, z = 0)$. For the sake of clarity in graphical presentation, we also scale the normalized intensities by the multiplicative factor $\exp(\tau)$.

In order to investigate the significance of the optical thickness, we calculated the power received by a coaxial detector of radius $R_D = 1$ cm. If $F(\theta_D, \vec{r}, \tau)$ denotes generically the beam intensity, then the received power is defined as

$$P(R_D) = 2\pi \int_0^{R_D} F(\theta_D, \vec{r}, \tau) r dr \quad (50)$$

The received power is also scaled by the multiplicative factor $\exp(\tau)$, and the power received at $z = 0$ is divided out. The numerical values were obtained for received power for a coaxial detector of diameter $R_D = 1$ cm, and the situation is depicted in Figs. 4-6 corresponding to the same parameters as in Figs. 1-4, respectively. As the FOV increases, both the intensity and the received power saturate rapidly, independently of the optical depth. This corresponds to the situation of an open detector. The contribution of the scattered power becomes dominant in the saturation region for optical depth of the order of 10.

Gaussian phase functions as given by Eq. (11) were best fitted in Ref. 8 to the exact Mie phase functions for monodisperse aerosols with radii in the range from 2.01 to 40.2 μm . In Figs. 7-9, we show the intensity vs. detector's FOV. In addition, we show the received power vs. FOV for $\tau = 4.0$ (Fig. 10). These sets of results were computed for the model particles characterized by the parameters $\alpha = 289.33 \text{ rad}^{-1}$, and

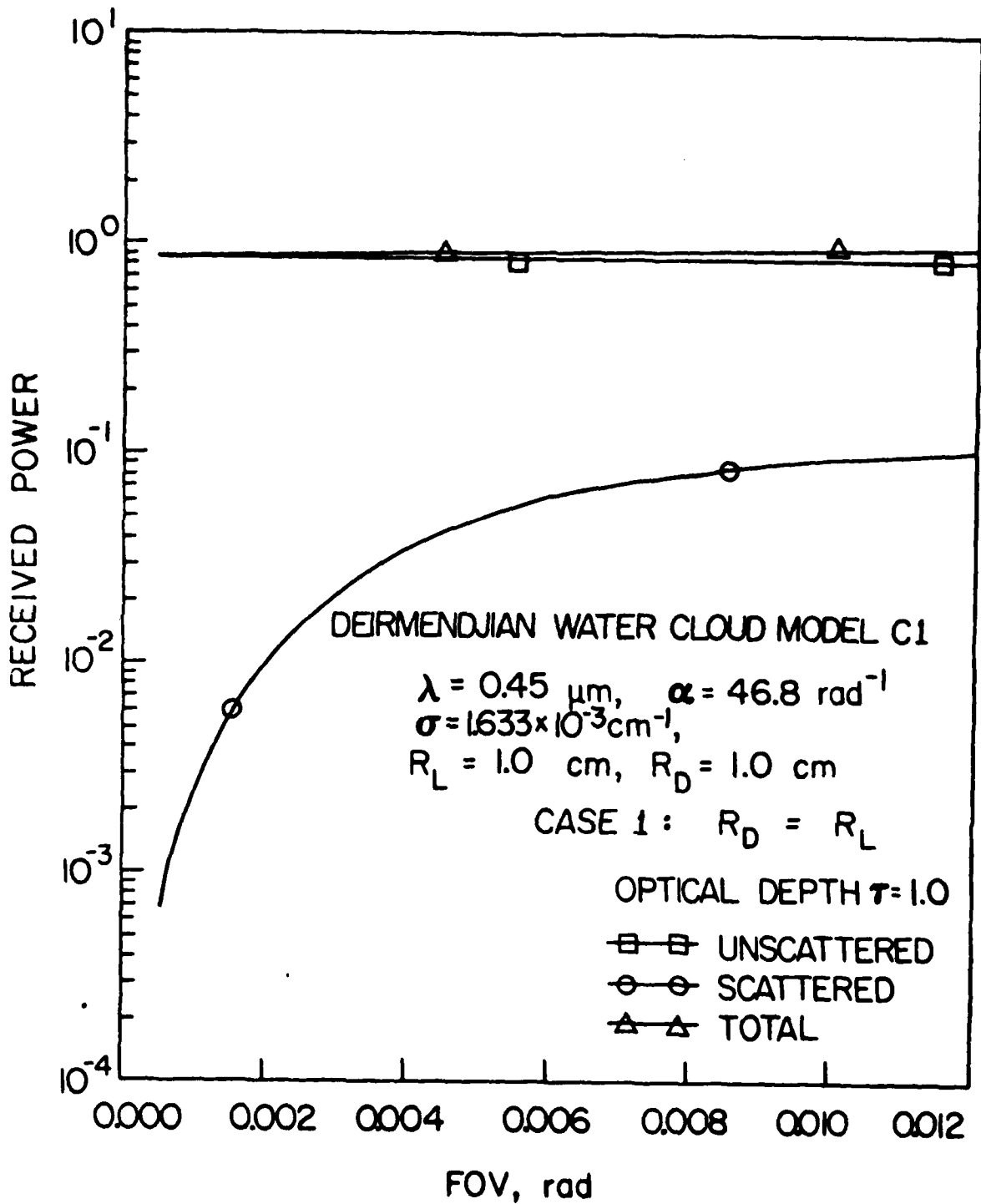


Figure 4. Received power (arbitrary units) on the beam axis as function of detector FOV corresponding to $\alpha = 46.80 \text{ rad}^{-1}$, $R_D = 1.0 \text{ cm}$, and $\tau = 1.0$.

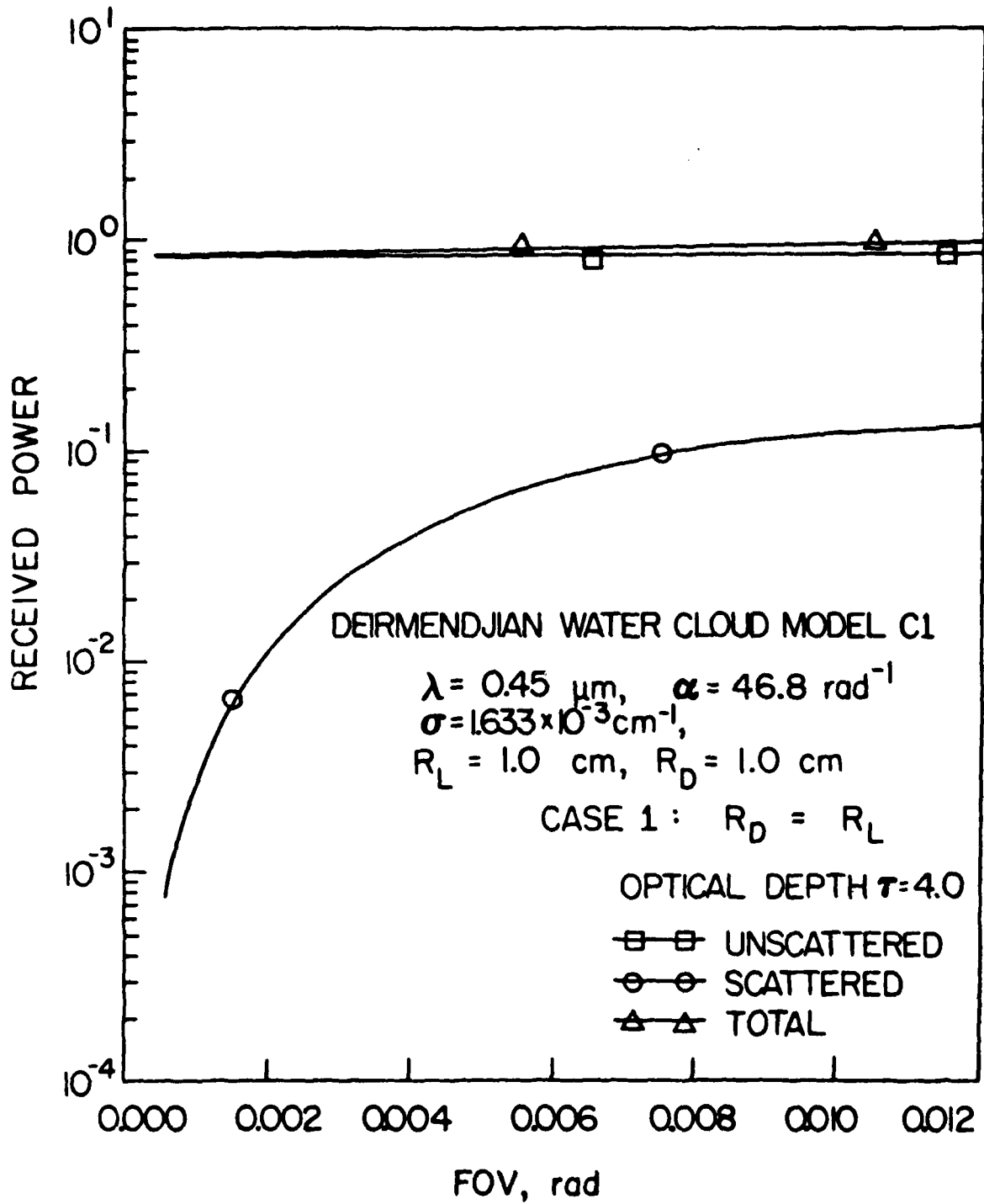


Figure 5. Received power (arbitrary units) on the beam axis as function of detector FOV corresponding to $\alpha = 46.80 \text{ rad}^{-1}$, $R_D = 1.0 \text{ cm}$, and $\tau = 4.0$.

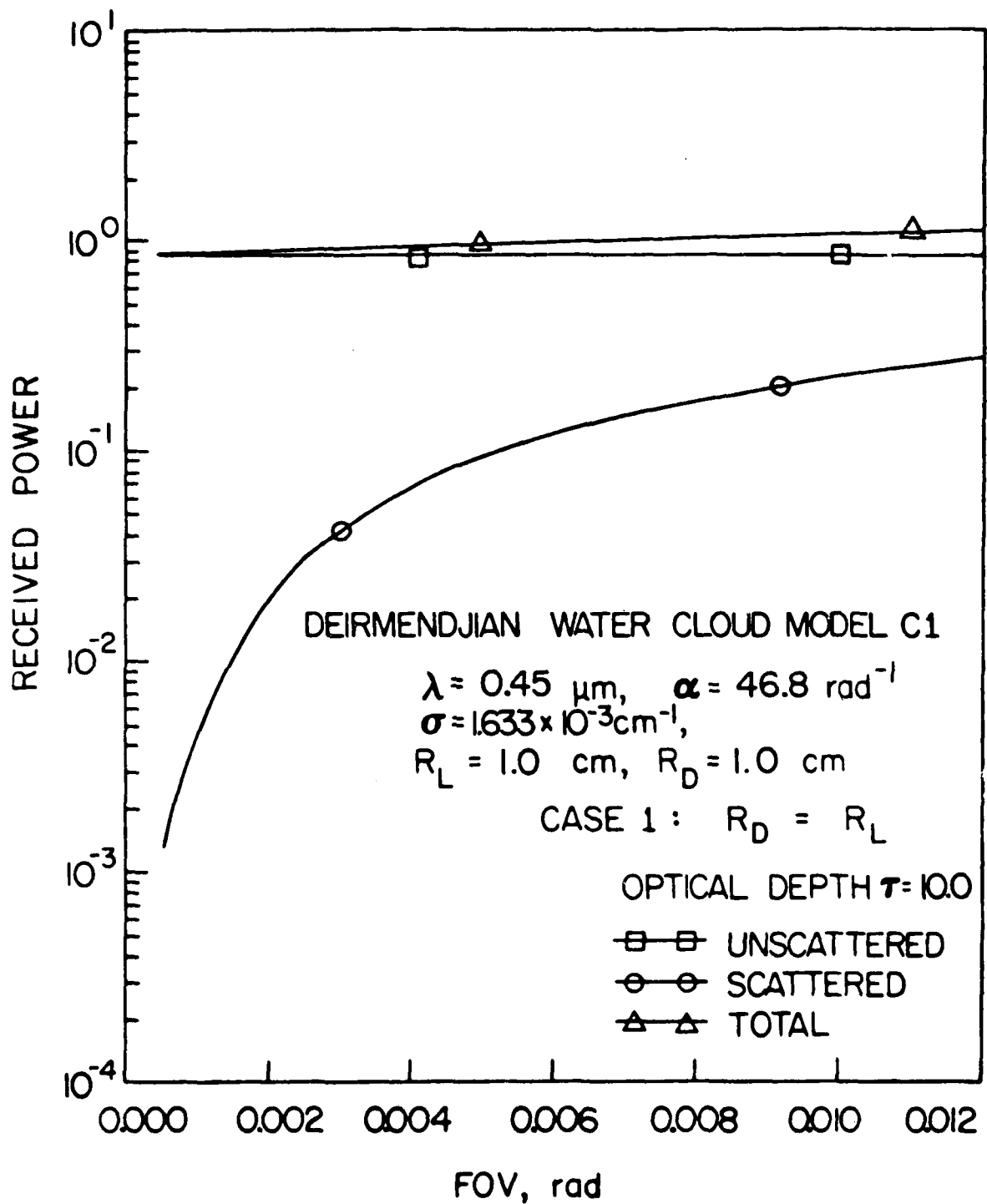


Figure 6. Received power (arbitrary units) on the beam axis as function of detector FOV corresponding to $\alpha = 46.80 \text{ rad}^{-1}$, $R_D = 1.0 \text{ cm}$, and $\tau = 10.0$

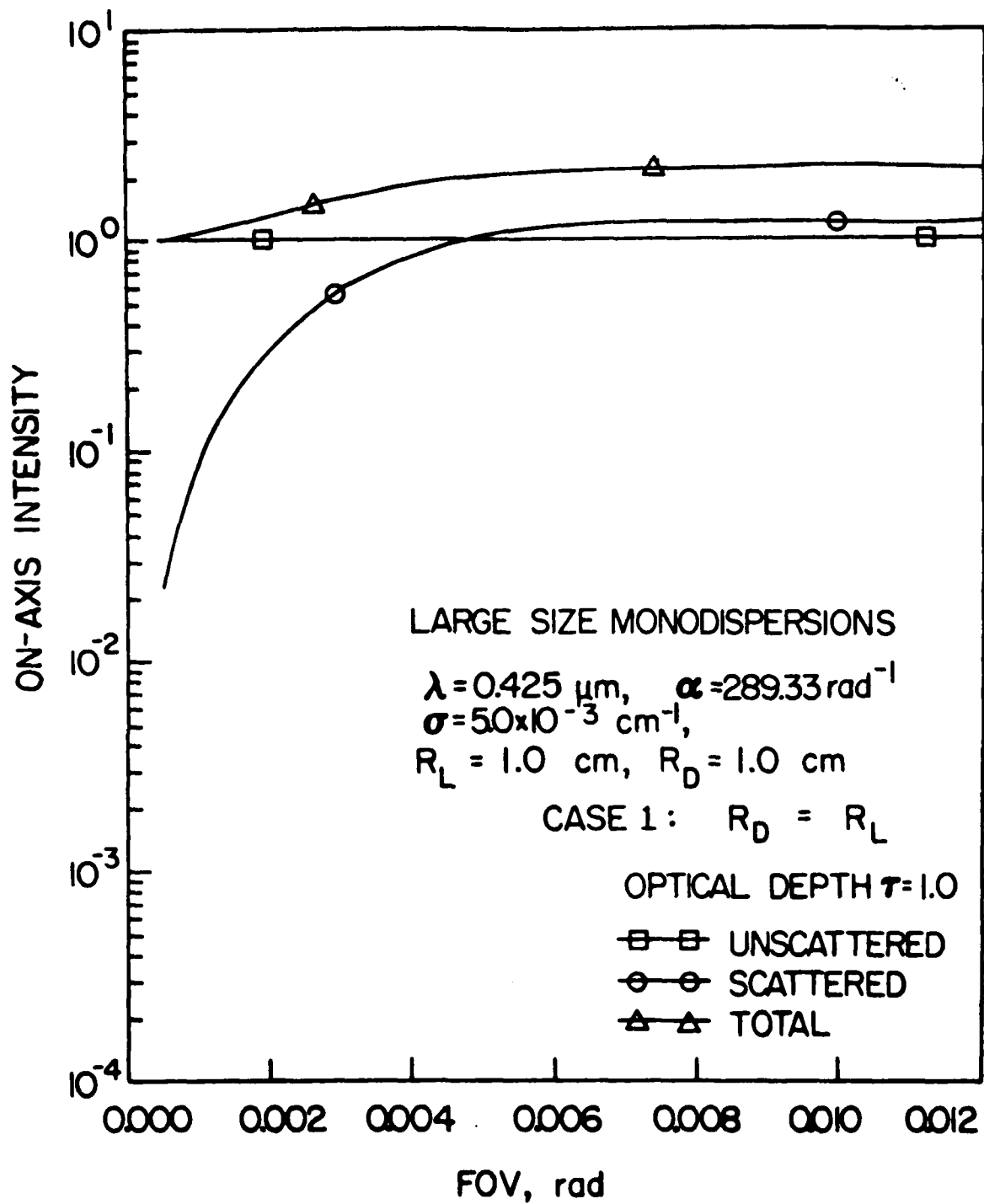


Figure 7. Normalized intensity on the beam axis as function of detector FOV corresponding to $\alpha = 289.33 \text{ rad}^{-1}$, $R_D = 1.0 \text{ cm}$, and $\tau = 1.0$.

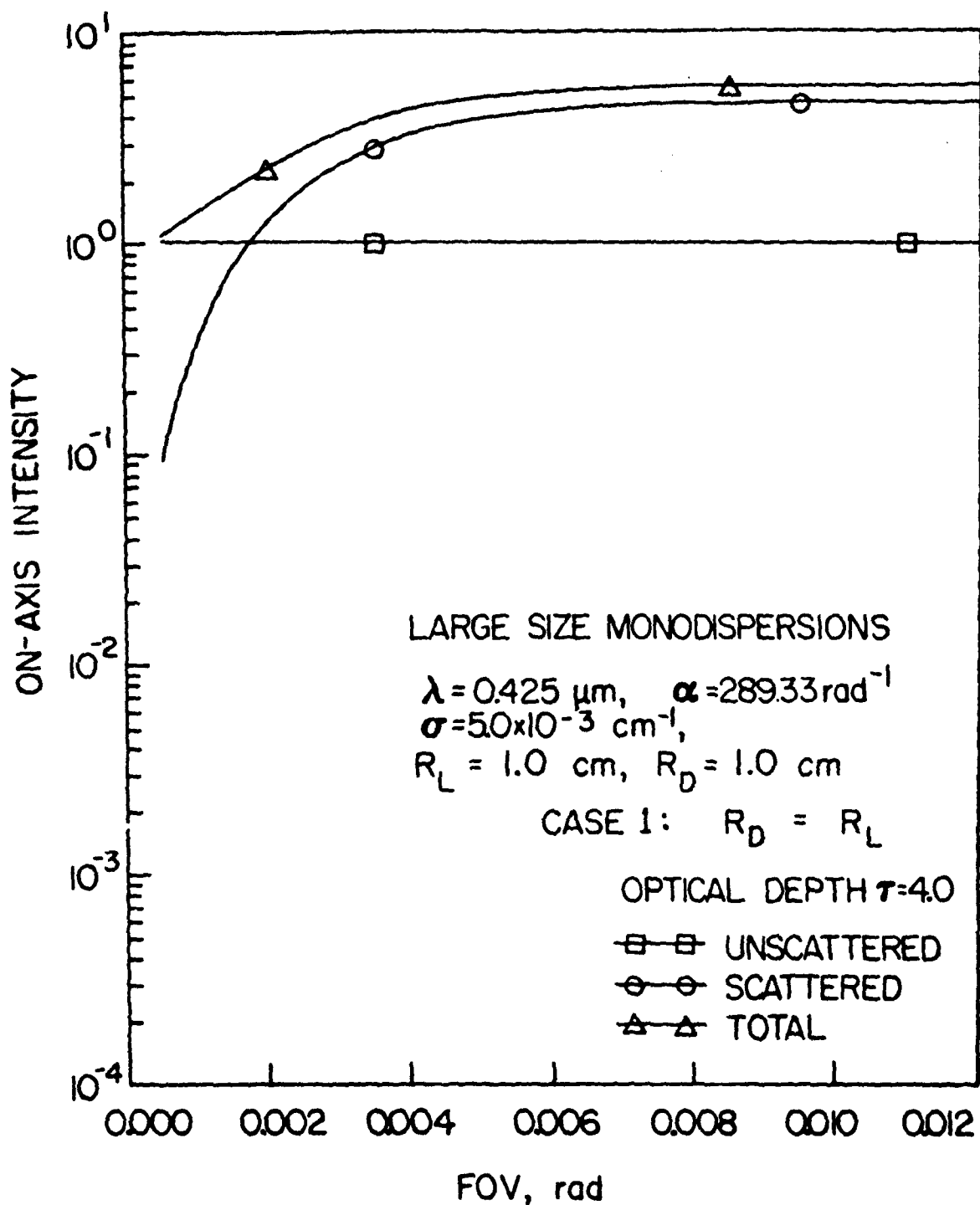


Figure 8. Normalized intensity on the beam axis as function of detector FOV corresponding to $\alpha = 289.33 \text{ rad}^{-1}$, $R_D = 1.0 \text{ cm}$, and $\tau = 4.0$.

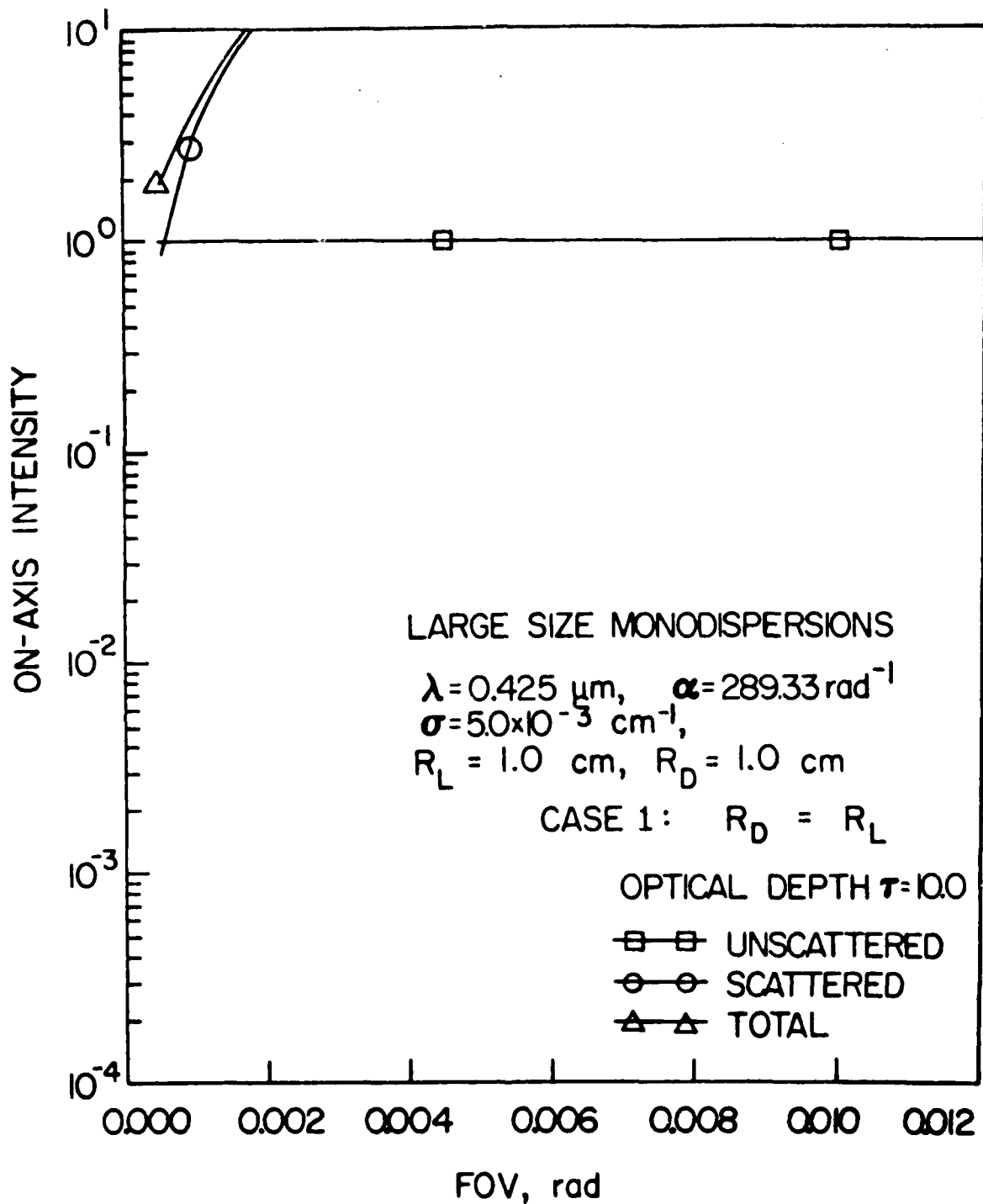


Figure 9. Normalized intensity on the beam axis as function of detector FOV corresponding to $\alpha = 289.33 \text{ rad}^{-1}$, $R_D = 1.0 \text{ cm}$, and $\tau = 10.0$.

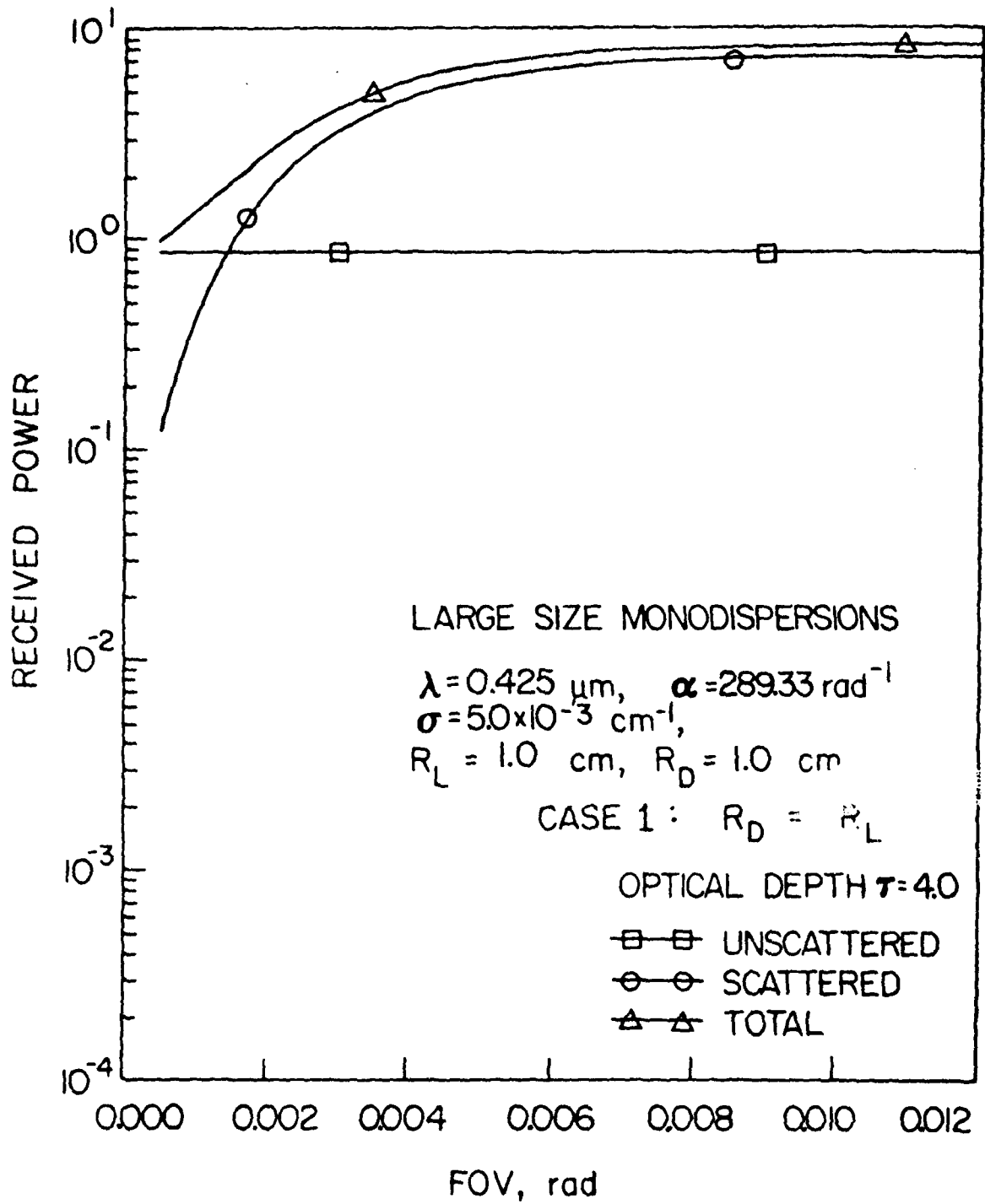


Figure 10. Received power (arbitrary units) on the beam axis as function of detector FOV corresponding to $\alpha = 289.33 \text{ rad}^{-1}$, $R_D = 1.0 \text{ cm}$, and $\tau = 4.0$. Received power is multiplied by $\exp(\tau)$.

$\sigma = 5.0 \times 10^{-2} \text{ cm}^{-1}$ at $\lambda = 0.45 \text{ }\mu\text{m}$, for a coaxial detector of diameter $R_D = 1 \text{ cm}$. Note that the phase function and the Gaussian fit to the forward lobe of the Mie phase function are plotted in Fig. 3 of Ref. 8.

In order to study the effect of the detector's radius R_D , we let R_D assume values smaller and larger than the beam diameter of the 1.0 cm, viz, $R_D = 0.2 \text{ cm}$ and 2.0 cm . Results were obtained for the same parameters as in the case of $R_D = 1.0 \text{ cm}$. However, for the sake of clarity we present only the results for $\tau = 4.0$ for the two cases, viz, $R_D = 0.2 \text{ cm}$ (Figs. 11-12) and $R_D = 2.0 \text{ cm}$ (Figs. 13-14). Figures 11-12 depict the corresponding values of intensity and received power as functions of FOV for $R_D = 0.2 \text{ cm}$, whereas, Figs. 13-14 depict the corresponding values for $R_D = 2.0 \text{ cm}$. The three cases ($R_D = 1.0, 0.2$ and 2.0 cm ; $\tau = 4.0$) for large particles with phase function parameter $\alpha = 289.33 \text{ cm}^{-1}$ show clearly the contrast in the behavior of the intensity and the received power.

The Fante-Dolin approximation employed in this paper enables one to estimate the corrections to the Bouguer-Beer law for a receiver having a finite field of view, as for example in Ref. 25.

VI. RECOMMENDATIONS

1. It should be noted that the small-angle approximation is valid for highly forward-peaked phase functions. It is, therefore, recommended that approaches be developed to deal with the case of MS in laser beams traversing small size aerosol particles, with broadly-peaked phase functions.

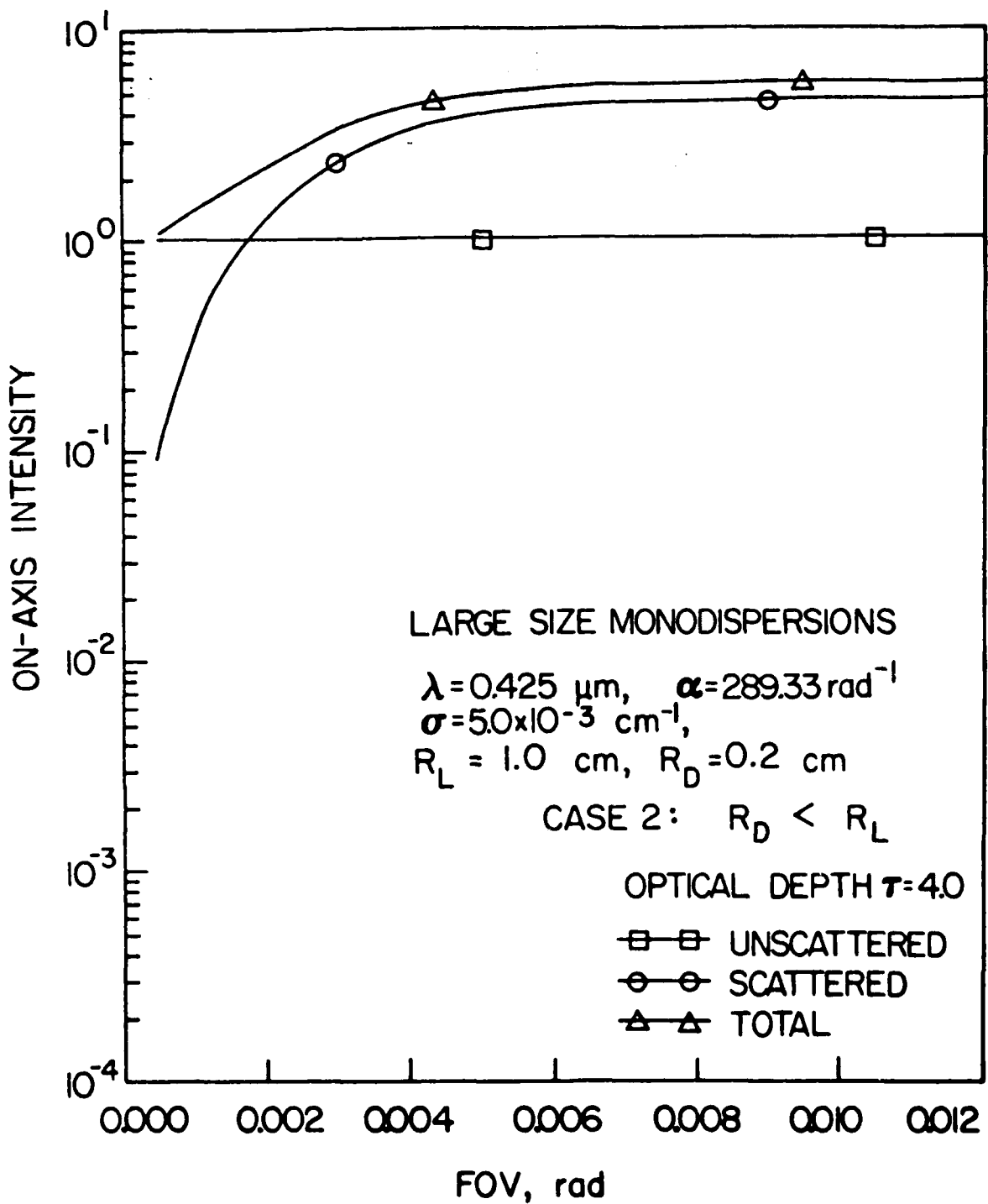


Figure 11. Normalized intensity on the beam axis as function of detector FOV for the same parameters as in Fig. 8 except $R_D = 0.2 \text{ cm}$.

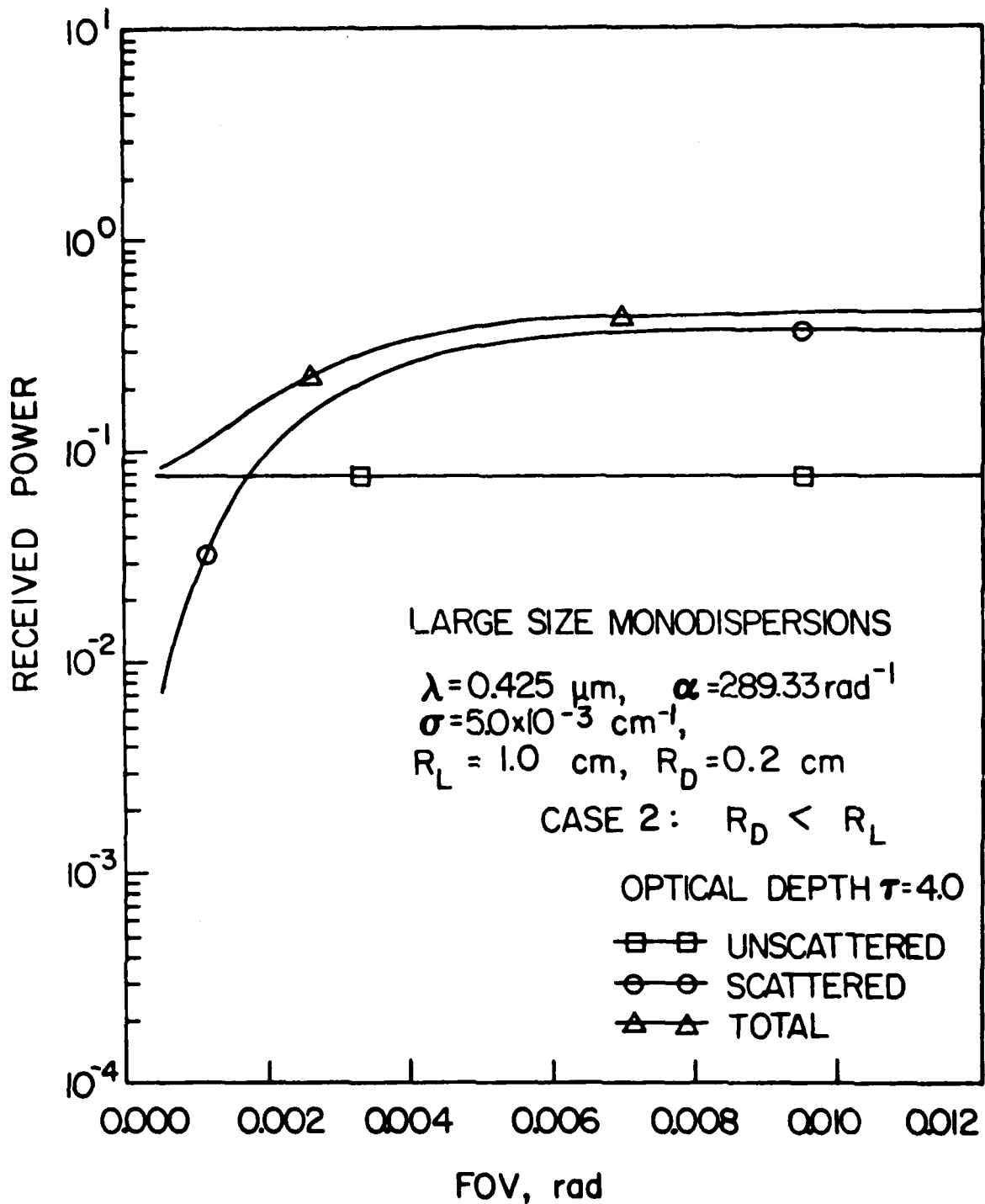


Figure 12. Received power (arbitrary units) on the beam axis as a function of detector FOV, for the same parameters as in Fig. 11. The received power is multiplied by $\exp(\tau)$.

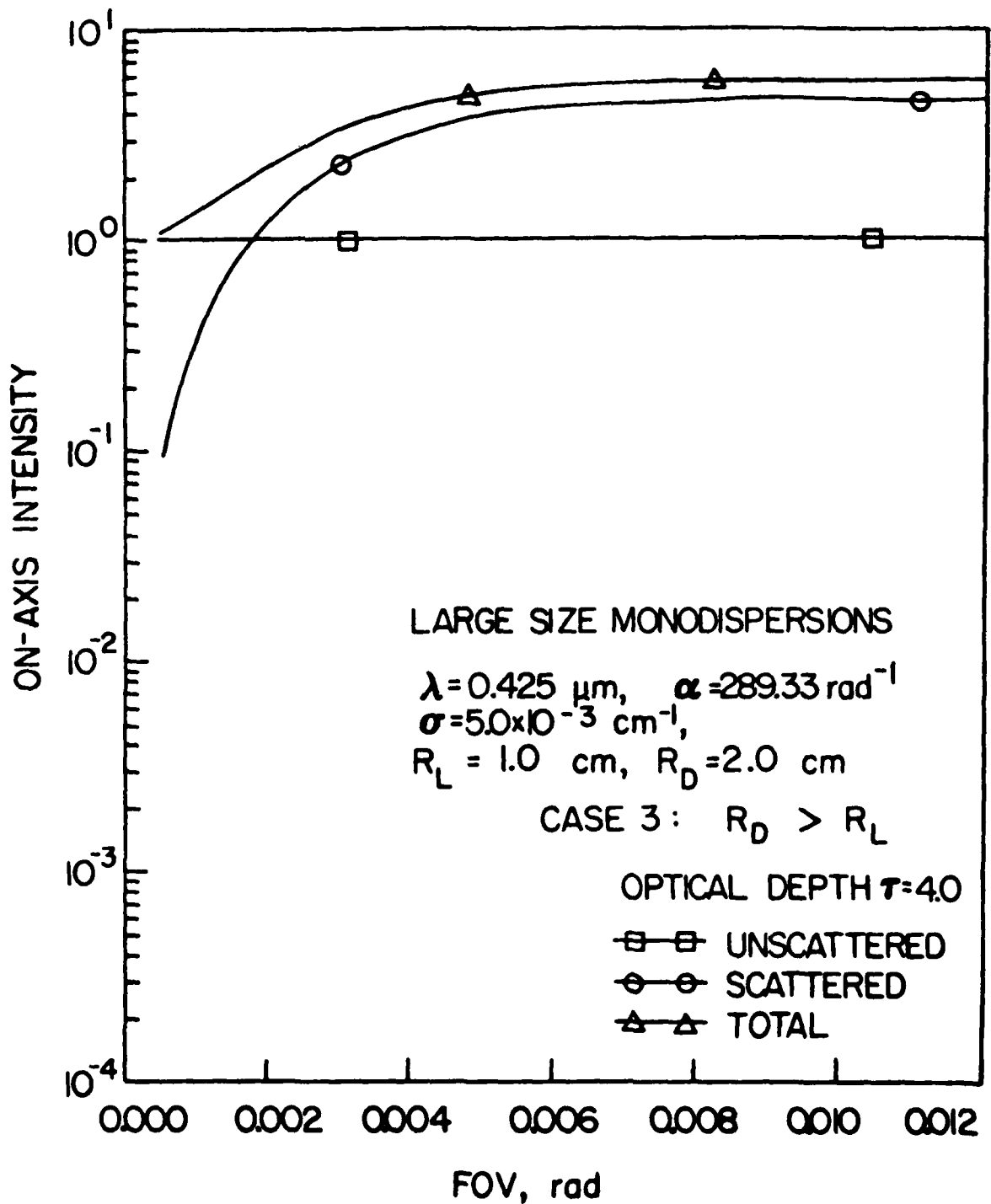


Figure 13. Normalized intensity on the beam axis as function of detector FOV for the same parameters as in Fig. 8 except $R_D = 2.0 \text{ cm}$.

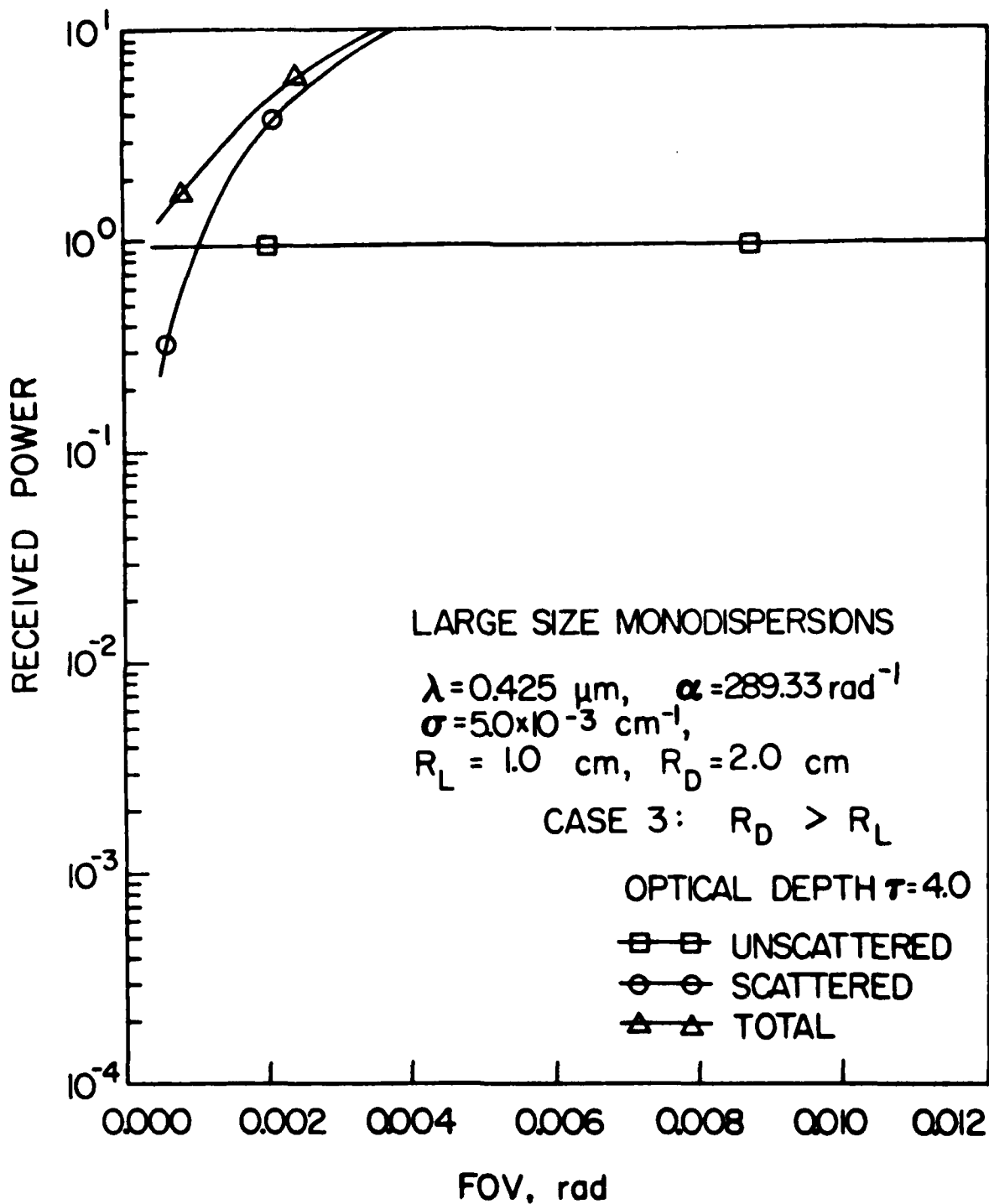


Figure 14. Received power (arbitrary units) on the beams axis as a function of detector FOV, for the same parameters as in Fig. 13. The received power is multiplied by $\exp(\tau)$.

2. It is recommended that experiments and numerical computations be performed to (a) determine the effects of the detector field of view on both the extinction and backscattering function measurements and (b) investigate the effects of beam diameter on optical extinction measurements.

3. It is recommended that the above investigation be repeated for the case of backscattering, which is of great importance for single-ended electro-optical systems.

BLANK

LITERATURE CITED

1. G. K. Goedecke, in EOSAEL 80, Vol. I, Technical Documentation, (L. D. Duncan, ed.), Atmospheric Sciences Laboratory Report ASL-TR-0072, January 1981.
2. E. A. Bucher, *Appl. Opt.* 12, 2391 (1973).
3. G. N. Plass and G. Kattawar, *Appl. Opt.* 7, 415 (1968).
4. W. G. Tam and A. Zardecki, *J. Opt. Soc. Am.* 69, 68 (1979).
5. A. Zardecki and W. G. Tam, *Can. J. Phys.* 57, 1301 (1979).
6. R. E. Jensen, *J. Opt. Soc. Am.* 70, 1557 (1980).
7. M. A. Box and A. Deepak, *J. Opt. Soc. Am.* 71, 1534 (1981).
8. A. Deepak, U. O. Farrukh, and A. Zardecki, *Appl. Opt.* 21, 431 (1982).
9. A. Deepak, A. Zardecki, U. O. Farrukh and M. A. Box, Proc. Workshop on Atmospheric Aerosols, Baltimore, MD 1979 (Spectrum Press, Hampton, VA) (1981).
10. A. Ishimaru, *Proc. IEEE* 65, 1030 (1977).
11. A. Ishimaru, *Wave Propagation and Scattering in Pandom Media*, Academic Press, New York (1978).
12. R. O. Gumprecht and C. M. Sliepcevich, *J. Phys. Chem.* 57, 90 (1953).
13. R. O. Gumprecht and C. M. Sliepcevich, *J. Phys. Chem.* 57, 95 (1953).
14. V. E. Zuev, M. V. Kabanov and B. A. Savelev, *Izv. Atm. and Oceanic Phys.* 3, 724 (1967).
15. A. Deepak and O. H. Vaughan, *Appl. Opt.* 17, 374 (1978).

16. A. Deepak and M. A. Box, *Appl. Opt.* 17, 2900 (1978).
17. A. Deepak and M. A. Box, *Appl. Opt.* 17, 3168 (1978).
18. L. S. Dolin, *Izv. V.U.Z. Radiofizika* 9, 61 (1966).
19. R. L. Fante, *IEEE AP21*, 750 (1973).
20. R. L. Fante, *J. Opt. Soc. Am.* 64, 592 (1974).
21. R. L. Fante, *Proc. IEEE* 62, 1400 (1974).
22. R. L. Fante, *Proc. IEEE* 68, 1424 (1980).
23. W. G. Tam and A. Zardecki, *Opt. Acta* 26, 659 (1979).
24. D. Diermendjian, *Electromagnetic Scattering by Spherical Polydispersions*,
(American Elsevier, New York, 1969).
25. W. G. Tam and A. Zardecki, *Appl. Opt.* 21, 2405 (1982).

DISTRIBUTION LIST FOR ARCSL-CR-83039

Names	Copies	Names	Copies
CHEMICAL SYSTEMS LABORATORY			
ATTN: DRDAR-CLB	1	Advanced Research Projects Agency	1
ATTN: DRDAR-CLB-C	1	1400 Wilson Boulevard	
ATTN: DRDAR-CLC-P	1	Arlington, VA 22209	
ATTN: DRDAR-CLB-PS	4	DEPARTMENT OF THE ARMY	
ATTN: DRDAR-CLB-R	1	HQDA	
ATTN: DRDAR-CLB-T	1	ATTN: DAMO-NCC	1
ATTN: DRDAR-CLB-TE	1	ATTN: DAMO-NC/COL Robinson (P)	1
ATTN: DRDAR-CLC-B	1	WASH DC 20310	
ATTN: DRDAR-CLC-C	1	HQ DA	
ATTN: DRDAR-CLF	1	Office of the Deputy Chief of Staff for	
ATTN: DRDAR-CLJ-R	1	Research, Development & Acquisition	
ATTN: DRDAR-CLJ-L	2	ATTN: DAMA-CSS-C	1
ATTN: DRDAR-CLJ-M	1	Washington, DC 20310	
ATTN: DRDAR-CLN	1	HQ Sixth US Army	
ATTN: DRDAR-CLN-S	1	ATTN: AFKC-OP-NBC	1
ATTN: DRDAR-CLN-ST	1	Presidio of San Francisco, CA 94129	
ATTN: DRDAR-CLT	1	Commander	
ATTN: DRDAR-CLY-A (Pennsyle, Hundley)	2	DARCOM, STITEUR	
ATTN: DRDAR-CLY-R	1	ATTN: DRXST-ST1	1
COPIES FOR AUTHOR(S)		Box 48, APO New York 09710	
Research Division	10	Commander	
RECORD COPY: DRDAR-CLB-A	1	USASTCFEO	
DEPARTMENT OF DEFENSE			
Defense Technical Information Center		ATTN: MAJ Mikeworth	1
ATTN: DTIC-DDA-2	2	APO San Francisco 96328	
Cameron Station, Building 5		Army Research Office	
Alexandria, VA 22314		ATTN: DRXRO-CB (Dr. R. Ghirardelli)	1
Director		ATTN: DRXRO-GS	1
Defense Intelligence Agency		ATTN: Dr. W. A. Flood	1
ATTN: DB-4G1	1	P.O. Box 12211	
Washington, DC 20301		Research Triangle Park, NC 27709	
Deputy Under Secretary of Defense for		HQDA ODUSA (OR)	
Research and Engineering (R&E)		ATTN: Dr. H. Fallin	1
ATTN: Dr. Musa	1	Washington, DC 20310	
ATTN: COL Friday	1	HQDA (DAMO-RQD)	
ATTN: COL Winter	1	ATTN: MAJ C. Collat	1
Washington, DC 20301		Washington, DC 20310	
Defense Advanced Research Projects Agency			
ATTN: Dr. Tegnella	1		
Washington, DC 20301			

HQDA, OCE
ATTN: DAEN-RDM (Dr. Gomez) 1
Massachusetts Ave, NW
Washington, DC 20314

OFFICE OF THE SURGEON GENERAL

Commander
US Army Medical Research and
Development Command
ATTN: SGRD-UBG (Mr. Eaton) 1
ATTN: SGRD-UBG-OT (CPT Johnson) 1
ATTN: LTC Don Gensler 1
Fort Detrick, MD 21701

Commander
US Army Medical Bioengineering Research
and Development Laboratory
ATTN: SGRD-UBD-AL, Bldg 568 1
Fort Detrick, Frederick, MD 21701

Commander
USA Medical Research Institute of
Chemical Defense
ATTN: SGRD-UV-L 1
Aberdeen Proving Ground, MD 21010

US ARMY MATERIEL DEVELOPMENT AND
READINESS COMMAND

Commander
US Army Materiel Development and
Readiness Command
ATTN: DRCDE-DM 1
ATTN: DRCLDC 1
ATTN: DRCMT 1
ATTN: DRCSF-P 1
ATTN: DRCSF-S 1
ATTN: DRCDL (Mr. N. Klein) 1
ATTN: DRCBSI-EE (Mr. Giambalvo) 1
ATTN: DRCMDM-ST (Mr. T. Shirata) 1
5001 Eisenhower Ave
Alexandria, VA 22333

Commander
US Army Foreign Science & Technology Center
ATTN: DRXST-MT3 1
ATTN: DRXST-MT3 (Poleski) 1
220 Seventh St., NE
Charlottesville, VA 22901

Director
DARCOM Field Safety Activity
ATTN: DRXOS-SE (Mr. Yutmeyer) 1
Charlestown, IN 47111

PM Smoke/Obscurants
ATTN: DRCPM-SMK-E (A. Van de Wal) 1
ATTN: DRCPM-SMK-M 1
ATTN: DRCPM-SMK-T 1
Aberdeen Proving Ground, MD 21005

Director
US Army Materiel Systems Analysis Activity
ATTN: DRXSY-MP 1
ATTN: DRXSY-CA (Mr. Metz) 1
ATTN: DRXSY-FJ (J. O'Bryon) 1
ATTN: DRXSY-GP (Mr. Fred Campbell) 1
Aberdeen Proving Ground, MD 21005

USA AVIATION RESEARCH AND
DEVELOPMENT COMMAND

Director
Applied Technology Lab
USARTL (AVRADCOM)
ATTN: DAVDL-ATL-ASV 1
ATTN: DAVDL-ATL-ASW 1
ATTN: DAVDL-EV-MOS (Mr. Gilbert) 1
Ft. Eustis, VA 23604

Commander
USA Avionics R&D Activity
ATTN: DAVAA-E(M. E. Sonatag) 1
Ft. Monmouth, NJ 07703

USA MISSILE COMMAND

Commander
US Army Missile Command
Director, Energy Directorate
ATTN: DRSMI-RHFT 1
ATTN: DRSMI-RMST 1
ATTN: DRSMI-YLA (N. C. Katos) 1
Redstone Arsenal, AL 35809

Commander
US Army Missile Command
Redstone Scientific Information Center
ATTN: DRSHI-REO (Mr. Widenhofer) 1
ATTN: DRSMI-RGT (Mr. Matt Maddix) 1
ATTN: DRDMI-CGA (Dr. B. Fowler) 1
ATTN: DRDMI-KL (Dr. W. Wharton) 1
ATTN: DRDMI-TE (Mr. H. Anderson) 1
Redstone Arsenal, AL 35809

Commander
 US Army Missile Command
 Redstone Scientific Information Center
 ATTN: DRSMI-RPR (Documents) 1
 Redstone Arsenal, AL 35809

USA COMMUNICATIONS-ELECTRONICS COMMAND

Commander
 USA Communications-Electronics Command
 ATTN: DRSEL-WL-S (Mr. J. Charlton) 1
 Ft. Monmouth, NJ 07703

Commander
 USA Electronics Research and
 Development Command
 ATTN: DRDEL-CCM (Dr. J. Scales) 1
 ATTN: DELHD-RT-CB (Dr. Sztankay) 1
 Adelphi, MD 20783

Commander
 Harry Diamond Laboratories
 ATTN: DRXDO-RCB (Dr. Donald Wortman) 1
 ATTN: DRXDO-RCB (Dr. Clyde Morrison) 1
 ATTN: DRXDO-RDC (Mr. D. Giglio) 1
 2800 Powder Mill Road
 Adelphi, MD 20783

Commander
 USA Materials & Mechanics Research Center
 ATTN: DRXMR-KA (Dr. Saul Isserow) 1
 Watertown, MA 02172

Commander
 USA Cold Region Research Engineering Laboratory
 ATTN: George Aitken 1
 Hanover, NH 03755

Commander/Director
 Combat Surveillance and Target
 Acquisition Laboratory
 ERADCOM
 ATTN: DELCS-R (E. Frost) 1
 Ft. Monmouth, NJ 07703

Director
 Atmospheric Sciences Laboratory
 ATTN: DELAS-AS (Dr. Charles Bruce) 1
 ATTN: DELAS-AS-P (Mr. Tom Pries) 1
 ATTN: DELAS-EO-EN (Dr. Donald Snider) 1
 ATTN: DELAS-EO-EN (Mr. James Gillespie) 1
 ATTN: DELAS-EO-ME (Dr. Frank Niles) 1
 ATTN: DELAS-EO-ME (Dr. Ronald Pinnick) 1
 ATTN: DELAS-EO-MO (Dr. Melvin Heaps) 1
 ATTN: DELAS-EO-MO (Dr. R. Sutherland) 1
 ATTN: DELAS-EO-S (Dr. Louis Duncan) 1
 White Sands Missile Range, NM 88002

US ARMY ARMAMENT RESEARCH AND
 DEVELOPMENT COMMAND

Commander
 US Army Armament Research and
 Development Command
 ATTN: DRDAR-LCA-L 1
 ATTN: DRDAR-LCE (Mr. Scott Morrow) 1
 ATTN: DRDAR-LCE-C 1
 ATTN: DRDAR-LCU-CE 1
 ATTN: DRDAR-NC (COL Lymn) 3
 ATTN: DRDAR-SCA-T 1
 ATTN: DRDAR-SCF 1
 ATTN: DRDAR-SCP 1
 ATTN: DRDAR-SCS 1
 ATTN: DRDAR-TDC (Dr. D. Gyorog) 1
 ATTN: DRDAR-TSS 2
 ATTN: DRCPM-CAWS-AM 1
 Dover, NJ 07801

US Army Armament Research and
 Development Command
 ATTN: DRDAR-TSE-0A (Robert Thresher) 1
 National Space Technology Laboratories
 NSTL Station, MS 39529

Requirements and Analysis Office
 Foreign Intelligence and Threat
 Projection Division
 ATTN: DRDAR-RAI-C 1
 Aberdeen Proving Ground, MD 21010

Commander
 ARRADCOM
 ATTN: DRDAR-QAC-E 1
 Aberdeen Proving Ground, MD 21010

Director USA Ballistic Research Laboratory ARRADCOM ATTN: DRDAR-BLB ATTN: DRDAR-TSB-S Aberdeen Proving Ground, MD 21005	1 1	Commander USA Combined Arms Center and Fort Leavenworth ATTN: ATZL-CAM-IM Fort Leavenworth, KS 66027	1
US ARMY ARMAMENT MATERIEL READINESS COMMAND		Commander US Army Infantry Center ATTN: ATSH-CD-MS-C ATTN: ATSH-CD-MS-F ATTN: ATZB-DPT-PO-NBC Fort Benning, GA 31905	1 1 1
Commander US Army Armament Materiel Readiness Command ATTN: DRSAR-ASN ATTN: DRSAR-IRI-A ATTN: DRSAR-LEP-L ATTN: DRSAR-SF Rock Island, IL 61299	1 1 1 1	Commander USA Training and Doctrine Command ATTN: ATCD-N ATTN: ATCD-TEC (Dr. M. Pastei) ATTN: ATCD-Z Fort Monroe, VA 23651	1 1 1
Commander US Army Dugway Proving Ground ATTN: Technical Library (Docu Sect) Dugway, UT 84022	1	Commander US Army Armor Center ATTN: ATZK-CD-MS ATTN: ATZK-PPT-PO-C Fort Knox, KY 40121	1 1
US ARMY TRAINING & DOCTRINE COMMAND		Commander US Army TRADOC System Analysis Activity ATTN: ATAA-SL ATTN: ATAA-TDB (L. Dominguez) White Sands Missile Range, NM 880u2	1 1 1
Commandant US Army Infantry School ATTN: CTDD, CSD, NBC Branch Fort Benning, GA 31905	1	Commander USA Field Artillery School ATTN: ATSF-GD-RA Ft. Sill, OK 73503	1 1
Commandant US Army Missile & Munitions Center and School ATTN: ATSK-CM Redstone Arsenal, AL 35809	1	Director USA Concepts Analysis Agency ATTN: MOCA-SMC (Hal Hock) 8120 Woodmont Avenue Bethesda, MD 20014	1
Commander US Army Logistics Center ATTN: ATCL-MG Fort Lee, VA 23801	1	Los Alamos National Laboratory ATTN: T-DOT, MS B279 (S. Gersti) Los Alamos, NM 87545	1
Commandant US Army Chemical School ATTN: ATZN-CM-C ATTN: ATZN-CM-AD ATTN: ATZN-CN-CDM (Dr. J. Scully) Fort McClellan, AL 36205	1 2 1		
Commander USAAVNC ATTN: ATZQ-D-MS Fort Rucker, AL 36362	1		

US ARMY TEST & EVALUATION COMMAND

Commander
 US Army Test & Evaluation Command
 ATTN: DRSTE-CM-F 1
 ATTN: DRSTE-CT-T 1
 ATTN: DRSTE-AD-M (Warren Baity) 1
 Aberdeen Proving Ground, MD 21005

Commander
 USA EPG
 ATTN: STEEP-MM-IS 1
 ATTN: STEEP-MT-DS (CPT Decker) 1
 Ft. Huachuca, AZ 85613

Commander
 Dugway Proving Ground
 ATTN: STEDP-MT (Dr. L. Solomon) 1
 Dugway, UT 84022

DEPARTMENT OF THE NAVY

Commander
 Naval Research Laboratory
 ATTN: Code 5709 (Mr. W. E. Howell) 1
 ATTN: Code 6532 (Mr. Curcio) 1
 ATTN: Code 6532 (Mr. Trusty) 1
 ATTN: Code 6530-2 (Mr. Gordon Stamm) 1
 ATTN: Code 8320 (Dr. Lothar Ruhnke) 1
 ATTN: Code 8326 (Dr. James Fitzgerald) 1
 ATTN: Code 43202 (Dr. Hermann Gerber) 1
 4555 Overlook Avenue, SW
 Washington, DC 20375

Chief, Bureau of Medicine & Surgery
 Department of the Navy
 ATTN: MED 3033 1
 Washington, DC 20372

Commander
 Naval Air Systems Command
 ATTN: Code AIR-301C (Dr. H. Rosenwasser) 1
 ATTN: Code AIR-5363 (D. C. Caldwell) 1
 Washington, DC 20361

Commander
 Naval Sea Systems Command
 ATTN: SEA-62Y13 (LCDR Richard Gilbert) 1
 ATTN: SEA-62Y21 (A. Kanterman) 1
 ATTN: SEA-62Y21 (LCDR W. Major) 1
 Washington, DC 20362

Project Manager
 Theatre Nuclear Warfare Project Office
 ATTN: TN-09C 1
 Navy Department
 Washington, DC 20360

Institute for Defense Analysis 1
 400 Army-Navy Drive
 Arlington, VA 22202

Commander
 Naval Surface Weapons Center
 Dahlgren Laboratory
 ATTN: DX-21 1
 ATTN: Mr. R. L. Hudson 1
 ATTN: F-56 (Mr. Douglas Marker) 1
 Dahlgren, VA 22448

Commander
 Naval Intelligence Support Center
 ATTN: Code 434 (H. P. St. Aubin) 1
 4301 Suitland Road
 Suitland, MD 20390

Commander
 Naval Explosive Ordnance Disposal
 Technology Center
 ATTN: AC-3 1
 Indian Head, MD 20640

Officer-In-Charge
 Marine Corps Detachment 1
 Naval Explosive Ordnance Disposal
 Technology Center
 Indian Head, MD 20640

Commander
 Naval Air Development Center
 ATTN: Code 2012 (Dr. Robert Helmbold) 1
 Warminster, PA 18974

Commander
 Naval Weapons Center
 ATTN: Code 382 (L. A. Mathews) 1
 ATTN: Code 3882 (Dr. C. E. Dinerman) 1
 ATTN: Code 3918 (Dr. Alex Shianta) 1
 China Lake, CA 93555

Commanding Officer
 Naval Weapons Support Center
 Applied Sciences Department
 ATTN: Code 50C, Bldg 190 1
 ATTN: Code 502 (Carl Lohkamp) 1
 Crane, IN 47522

US MARINE CORPS		AFOSR/NE	
Commanding General		ATTN: MAJ H. Winsor	1
Marine Corps Development and Education Command		Bolling AFB, DC 20332	
ATTN: Fire Power Division, D091	1	OUTSIDE AGENCIES	
Quantico, VA 22134		Battelle, Columbus Laboratories	
DEPARTMENT OF THE AIR FORCE		ATTN: TACTEC	1
Department of the Air Force		505 King Avenue	
Headquarters Foreign Technology Division		Columbus, OH 43201	
ATTN: TQTR	1	Toxicology Information Center, JH 652	
Wright-Patterson AFB, OH 45433		National Research Council	1
HQ AFCLC/LOWMM	1	2101 Constitution Ave., NW	
Wright-Patterson AFB, OH 45433		Washington, DC 20418	
AFAMRL/TS		Dr. W. Michael Farmer, Assoc Prof, Physics	
ATTN: COL Johnson	1	University of Tennessee Space Institute	1
Wright-Patterson AFB, OH 45433		Tullahoma, TN 37388	
HQ AFSC/SDZ	1	ADDITIONAL ADDRESSEES	
ATTN: CPT D. Riedlger		Office of Missile Electronic Warfare	
Andrews AFB, MD 20334		ATTN: DELEW-M-T-AC (Ms Arthur)	1
USAF TAWC/THL	1	White Sands Missile Range, NM 88002	
Eglin AFB, FL 32542		US Army Mobility Equipment Research and Development Center	
USAF SC		ATTN: DROME-RT (Mr. O. F. Kezer)	1
ATTN: AD/YQ (Dr. A. Vasiloff)	1	Fort Belvoir, VA 22060	
ATTN: AD/YQO (MAJ Owens)	1	Director	
Eglin AFB, FL 32542		US Night Vision and EO Laboratories	
AD/SRO	1	ATTN: DRSEL-NV-VI (Dr. R. G. Buser)	1
Eglin AFB, FL 32542		ATTN: DRSEL-NV-VI (Mr. R. Bergemann)	1
Dr. Charles Arpke	1	ATTN: DELNV-VI (Luanne Obert)	1
OSV Field Office		ATTN: DELNV-L (D. N. Spector)	1
P.O. Box 1925		Fort Belvoir, VA 23651	
Eglin AFB, FL 32542		Commandant	
Commander		Academy of Health Sciences, US Army	
Hanscom Air Force Base		ATTN: HSHA-SSI	2
ATTN: AFGL-POA (Dr. Frederick Volz)	1	Fort Sam Houston, TX 78234	
Bedford, MA 01731			
Headquarters			
Tactical Air Command			
ATTN: DRP	1		
Langley AFB, VA 23665			

	1
laboratories	1
Center, JH 652	1
icli	1
, NW	
Assoc Prof, Physics	
ie Space Institute	1
Electronic Warfare	
(s Arthur)	1
ange, NM 88002	
ment Research and	
r	
D. F. Kezer)	1
50	
D Laboratories	
r. R. G. Buser)	1
r. R. Bergemann)	1
ie Obert)	1
Spector)	1
31	
ances, US Army	2
78234	

END

DATE
FILMED

8 - 8

DTIC